YIELD DESIGN SOLUTIONS TO BEARING CAPACITY OF A COLUMN-REINFOCED SOIL FOUNDATION UNDER INCLINED LOADING

María Alicia Arévalos Burró

Samir Maghous

alicia.arevalos@ufrgs.br

samir.maghous@ufrgs.br

Federal University of Rio Grande do Sul

Osvaldo Aranha 99, 90035-190, Porto Alegre, Rio Grande do Sul, Brasil

Abstract. *Most design procedures devised to evaluating the bearing capacity of column-reinforced foundations have mainly dealt with foundations under vertical loading. The purpose of the present work is to investigate within the framework of limit analysis theory the ultimate bearing capacity problem of column-reinforced foundations under inclined loading. Special emphasis is given to the effect of reinforcement on the interaction diagram relating the foundation load components. Starting from the situation of an isolated column, a lower bound solution for the bearing capacity is derived by considering statically admissible piecewise linear stress fields that comply with the failure condition everywhere in the foundation soil. On the other hand, the kinematic approach of limit analysis makes it possible, through the implementation of failure mechanisms on the column-reinforced structure, to derive upper bound estimates of the bearing capacity for each value of the inclination angle of applied load. The semi-analytical expressions of both lower and upper bound estimates allow for a parametric study on the improvement of the bearing capacity as a function of dimensionless parameters, which are defined from geometrical and strength properties. In this context, design charts are presented to provide an insight into the reinforcement mechanism. Generalization of the approach to the situation of a soil reinforced by a group of columns is subsequently undertaken in the context of plane strain conditions. It is shown in particular that, as soon as the horizontal component of the force increases, the vertical component of the bearing capacity decreases, thus emphasizing the strong interaction between the load components.*

Keywords: *Bearing Capacity, Column Reinforcement, Foundations, Inclined Loading, Limit Analysis*

1   INTRODUCTION

The columns reinforcement technique consists in incorporating into a soft soil regularly spaced vertical cylindrical inclusions. Two categories may be devised depending on the column material: the "stone-column" and the "lime-cement column" techniques. The main improvement expected from these techniques is to reduce settlements of highly compressive soils, accelerate the stage of primary consolidation and increase bearing capacity. The present contribution is concerned with the latter issue.

The common method of stone-column has been used since 1970's (Datye and Madhav, 1988). The reinforcing material is a vibrocompacted stone or ballast exhibiting high frictional properties. It´s construction is made by using probes that vibrate in the horizontal direction and penetrates the ground (Schaeffer, 1997). On the other hand, lime-cement columns construction consists in blending the weak soil mass with dry lime and cement using a rotary tool to form treated columns (Schaeffer,1997).

From a practical engineering viewpoint, design of column-reinforced foundations turns to be a challenging task owing to the strong heterogeneity of the geo-composite resulting from the association of native soft soil and the reinforcing soil columns. The design procedures conceived to estimate bearing capacity improvement from this reinforcement technique (e.g. Bouassida and Hadhri, 1995; Nazari and Ghazavi, 2012; Jellali et al., 2005; Jellali et al., 2007; Bouassida et al., 2009; Hassen et al., 2013) have mainly dealt with foundations under vertical loading. The question may arise as to whether the soil is strengthened by the stone columns/lime-cement columns or not when the foundation is submitted to an inclined loading. The main purpose of this paper consists in studying the yield strength of soft foundation soils reinforced by columns, giving special attention to the interaction between the vertical and horizontal component of the external load.
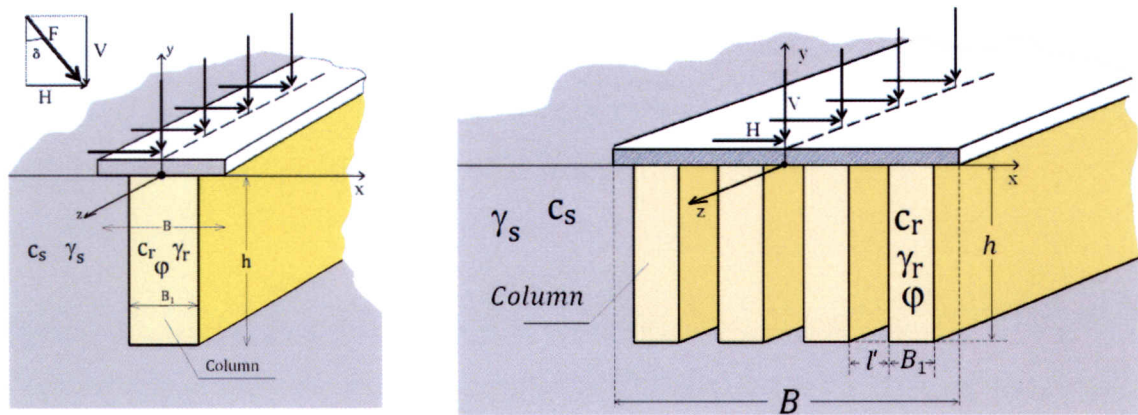
2   STATEMENT OF THE PROBLEM

The present work relates to the ultimate bearing capacity of a strip footing resting on the surface of a soft soil reinforced by columns. The foundation (width B) as well as the column (width B_1 and depth h), are assumed to have an infinite length following direction z (Fig.1), and therefore, the problem can be studied considering a plane strain situation. This foundation is subjected to uniformly distributed external inclined loads $\underline{F}$ along the z direction. It is also assumed to be rigid. The inclination angle of the load F with respect to the y axes is denoted by δ. Two situations are consecutively studied: the case of an isolated column and soil reinforced by a group of columns (Fig. 1).

The foundation soil and the reinforcement material (column) are modelled as *continuum media*. Each material is characterized by a strength-criterion which defines local failure. The soil underlying the foundation is generally a purely cohesive soft clay (for undrained considerations), whose strength capacities are described by a Tresca´s strength criterion with cohesion C_s. The reinforcement material (column) obeys a Coulomb's isotropic strength condition with cohesion C_r and friction angle φ. The gravity forces are considered in the analysis.

The problem defined above depends on a finite number of loading parameters: the vertical component V, the horizontal component H of the external force and the unit weight of each material (γ_r for the column material and γ_s for soil).

CILAMCE 2015

Proceedings of the XXXVI Iberian Latin-American Congress on Computational Methods in Engineering
Ney Augusto Dumont (Editor), ABMEC, Rio de Janeiro, RJ, Brazil, November 22-25, 2015

(a) The case of an isolated column   (b) The case of a group of columns

Figure 1. Strip footing resting on a column-reinforced soil

Dimensional arguments show that the ultimate load depends on the following dimensionless parameters:

$$n, \eta = nB_1 / B, \quad \xi = \gamma_s / (BC_s), \quad m = C_r / C_s, \quad \varphi, \quad k = \gamma_r / \gamma_s, \quad h / B, \quad l = l' / B \quad (1)$$

where n denotes to the column (trench) number and l' is the space between two neighboring columns (Fig.1). Results may also be expressed as a function of $a = (1 - l(n-1) - \eta)/2$.

3 LIMIT ANALYSIS FRAMEWORK

The problem is studied within the framework of limit analysis theory. The basic features of the yield design method are briefly outlined in this section. A detailed presentation may be found in Salençon (1990).

A lower bound solution (static approach) is derived by the construction of stress fields $\underline{\underline{\sigma}}$ that comply with the strength criteria everywhere in the soil and at the interface:

$$F \text{ is sustained} \Leftrightarrow \exists \begin{cases} \underline{\underline{\sigma}} \text{ statically admissible with } \underline{F} \\ f_s(\underline{\underline{\sigma}}) \leq 0 \text{ in the soil} \\ f_c(\underline{\underline{\sigma}}) \leq 0 \text{ in the columns} \end{cases} \quad (2)$$

where f_s and f_c are respectively the soil and column material strength criterion.

On the other hand, the much more frequently employed upper bound kinematic method uses the virtual work principle as a dualisation of the equilibrium conditions. This method is applied through the implementation of failure mechanisms on the column-reinforced structure. Virtual velocity fields $\underline{U}$ are then considered that involve either rigid body motions or structure strains.

The upper bound theorem of limit analysis states that a necessary condition for the system to remain safe under applied load $Q = \{F = (H,V), \gamma_s, \gamma_r\}$ is expressed by means the following inequality (Salençon, 1995):

$$W_{ex}(\underline{Q},\underline{U}) \leq W_{mr}(\underline{U}) \tag{3}$$

where W_{ex} is the rate of work performed by external forces in any velocity field $\underline{U}$ and W_{mr} is the maximum rate of work developed in the same velocity field $\underline{U}$. The so called maximum rate of work is defined as follows:

$$W_{mr}(\underline{U}) = \int_{\Omega} \pi(\underline{\underline{d}})d\Omega + \int_{\Sigma} \pi(n,[\underline{U}])d\Sigma \tag{4}$$

where $[\underline{U}]$ represents the velocity jump when crossing the discontinuity surface Σ along its unit normal $\underline{n}$ and $\underline{\underline{d}}$ the strain rate field associated with $\underline{U}$. The expression of the support function π appearing in Eq.(4) can be found in Salençon (1990) for Mohr-Coulomb and Tresca's strength criterion and depends on whether the velocity jump or strain rate is located in the soil or in the column.

For the Tresca soil material, condition $W_{mr}(\underline{U}) < +\infty$ requires that velocity jump $[\underline{U}]$ is tangential to the discontinuity surface. As regards the columns, $W_{mr}(\underline{U}) < +\infty$ requires that the velocity jump must be inclined at an angle equal to φ with respect to the discontinuity surface. Figure 2(a) sketches velocity jumps for a trench reinforced soil for plane discontinuity surfaces of the velocity field. In the case of a rigid body rotation, these conditions are translated in terms of cylindrical surfaces with a circular arc cross-section for the cohesive soil and a log-spiral curve cross-section of angle φ for the frictional material (Fig. 2(b)).

(a) Velocity jump for plane discontinuity surfaces

(b) Curve discontinuity surfaces for a rigid body rotation
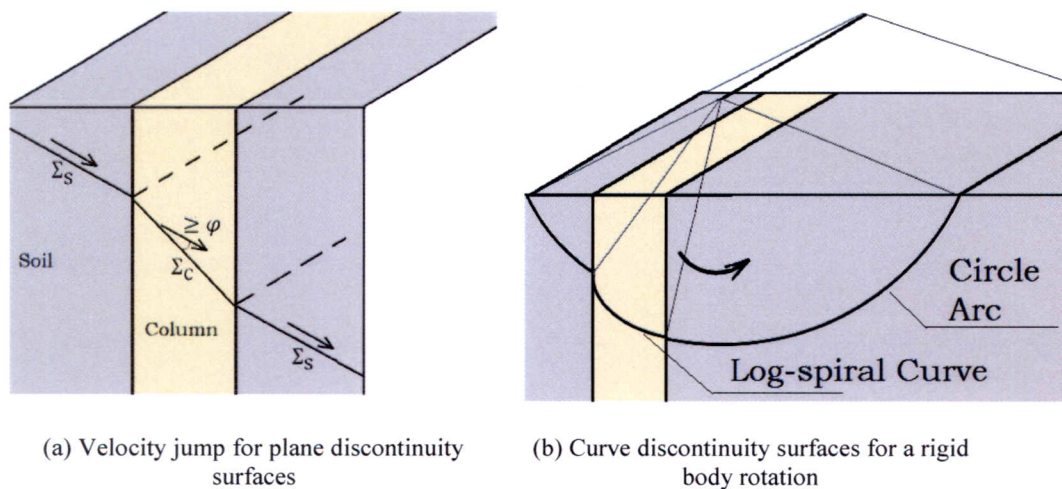
Figure 2. Velocity jump surfaces in a trench reinforced soil

The semi-analytical expressions of both lower and upper bound estimates allow for a parametric study on the improvement of the bearing capacity as a function of the dimensionless parameters of Eq. (1).

4 STATIC APPROACH

A static solution has been constructed, using a piecewise linear field as sketched in Fig. 3. In each one of the zones 1 to 3, the stress complies with the strength condition of constitutive material, namely the soil material (Tresca condition with cohesion C_s) and column material

CILAMCE 2015

Proceedings of the XXXVI Iberian Latin-American Congress on Computational Methods in Engineering
Ney Augusto Dumont (Editor), ABMEC, Rio de Janeiro, RJ, Brazil, November 22-25, 2015

(Mohr-Coulomb condition with cohesion C_r and frictional angle φ). The orientation of principal stress coincide with (x,y) directions in zones 1 and 4, while they depend on angle α in zones 2 and 3. Figure 3 (a) is referred to the case of an isolated column and Fig. 3 (b) to a foundation resting on a soil reinforced by a group of columns.
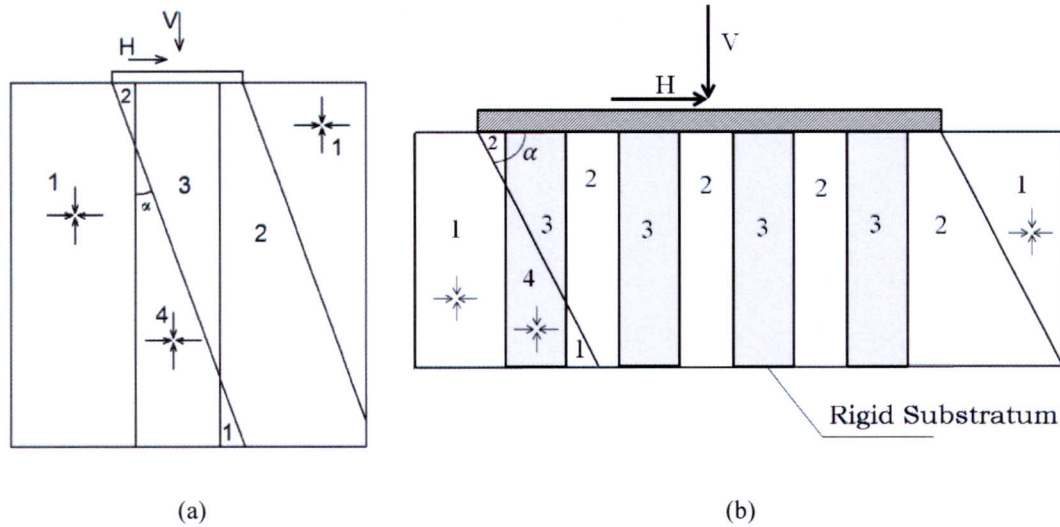

(a)   (b)

Figure 3. Piecewise linear stress field used for static approach

Referring to plane strain axes $x-y$ defined in Fig. 1, the stress field is defined by

$$\underline{\underline{\sigma}}_1 = \left(\gamma_s y - 2C_s\right) \underline{e}_x \otimes \underline{e}_x + \gamma_s y \, \underline{e}_y \otimes \underline{e}_y \tag{5}$$

$$\underline{\underline{\sigma}}_4 = \left(\gamma_s y - 2C_s\right) \underline{e}_x \otimes \underline{e}_x + \left(8C_s \cos^4\alpha - C_s 4\cos^2\alpha + A + \gamma_r y\right) \underline{e}_y \otimes \underline{e}_y \tag{6}$$

$$\underline{\underline{\sigma}}_2 = \begin{pmatrix} -C_s(1+2\cos 2\alpha - \cos 4\alpha) + \gamma_s y & C_s \sin 4\alpha \\ C_s \sin 4\alpha & -C_s(1+2\cos 2\alpha + \cos 4\alpha) + \gamma_s y \end{pmatrix} \tag{7}$$

$$\underline{\underline{\sigma}}_3 = \begin{pmatrix} -C_s(1+2\cos 2\alpha - \cos 4\alpha) + \gamma_s y & C_s \sin 4\alpha \\ C_s \sin 4\alpha & A + \gamma_r y \end{pmatrix} \tag{8}$$

where A is a constant determined by satisfying Mohr-Coulomb's strength criterion $\left(f_c(\underline{\underline{\sigma}}_3) \leq 0\right)$ in zone 3 for $0 \leq y \leq h$:

$$A = \min_{0 \leq y \leq h} \left\{ \frac{1}{\cos^2\varphi}\left((1+\sin^2\varphi)(\gamma_s y - C_s D) - \gamma_r y \cos^2\varphi - 2C_r \sin\varphi\cos\varphi - 2\sqrt{J}\right) \right\} \tag{9}$$

with $D = 1 + 2\cos 2\alpha - \cos 4\alpha$ and J given by:

$$J = C_s^2 D^2 \sin^2\varphi - 2C_s D\sin\varphi(\gamma_s y\sin\varphi - C_r\cos\varphi) + \gamma_s^2 y^2 \sin^2\varphi - 2y\gamma_s C_r \sin\varphi\cos\varphi + \left(C_r^2 - C_s^2\sin^2 4\alpha\right)\cos^2\varphi \tag{10}$$

with restrictions $0 \leq \alpha \leq 45°$ and $J \geq 0$. Mohr-Coulomb's strength condition is then numerically verified in zone 4 $\left(f_c(\underline{\underline{\sigma}}_4) \leq 0\right)$.

This stress field leads to the following lower bound solution:

$$F/_{BC_s} = \left(H/_{BC_s} = \sin 4\alpha, V/_{BC_s} = -\eta A/_{Cs} + (1-\eta)(1+2\cos 2\alpha + \cos 4\alpha)\right) \tag{11}$$

It is recalled that, for $\gamma_r \approx \gamma_s$, the loads $F_1 = (H = 0, V = (\pi + 2)BC_s)$ and $F_2 = (H = BC_s, V = 0)$ respectively derived by Prandtl (1923) and Salençon and Pecker (1995) for foundation lying on homogeneous cohesive soil, are lower bound solutions for the bearing capacity in the column reinforced situation soil for the case of a purely cohesive reinforcement material.

5 KINEMATIC APPROACH

This approach is based on the implementation of three failure mechanisms for the case of an isolated column and three failure mechanisms for the case of a group of columns.

5.1 The Case of an Isolated Column

Failure Mechanism I. The first mechanism displayed in Fig. 4 consists in a translational motion of the volumes $A'AEG$ and ADC, while the velocity $\underline{U} = U\,\underline{e}_\theta$ is constant and orthoradial in the fan AEC. This failure mechanism involves velocity jumps along lines $A'G$, GE, AE, CD and circular arc EC.
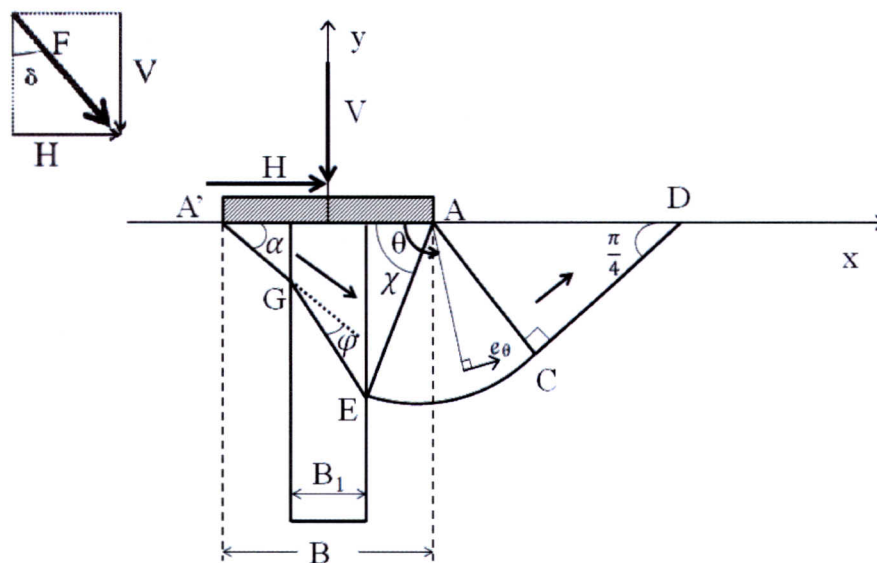

Figure 4. Generalized Prandtl type failure mechanism I

The rate of work $W_{ex}^{(F)}$ performed by the external force F is obtained by:

$$W_{ex}^{(F)} = UF\sin(\alpha + \delta) \tag{12}$$

where δ is used to denote the inclination angle of applied load (Fig. 4) and U represents the virtual velocity of volume $A'AEG$. The rate of work $W_{ex}^{(\gamma_s, \gamma_r)}$ performed by the gravity forces can be written as:

$$W_{ex}^{(\gamma_s, \gamma_r)} = \frac{1}{4}UB^2\gamma_s(1-\eta)\left[\sin\alpha\left(\tan\alpha(1-\eta) + \eta\tan(\alpha + \varphi) + 2k\eta\left(\tan\alpha + \eta\tan(\alpha + \varphi)\right)\right) - \frac{1}{2}A(1-\eta)\sin\chi\right] \tag{13}$$

with parameter $A = 1 + \left(\tan\alpha + \dfrac{2\eta\tan(\alpha+\varphi)}{1-\eta} \right)^2$ and $\tan\chi = \tan\alpha + \dfrac{2\eta}{1-\eta}\tan(\alpha+\varphi)$. Meanwhile the maximum resisting work is obtained by using Eq. 4, yielding:

$$W_{mr}(\underline{U}) = \frac{1}{2}C_s UB(1-\eta)\left(\frac{1}{\cos\alpha} + \left((1+3\pi/2-2\chi)\sin(\chi+\alpha)-\cos(\chi+\alpha)\right)\sqrt{A} \right) + \frac{C_s UBm\eta\cos\varphi}{\cos(\alpha+\varphi)} \tag{14}$$

Applying the fundamental kinematic equality, Eq. (3), yields

$$\frac{F}{BC_s} \leq \min_{\alpha} \frac{f(\alpha)}{\sin(\alpha+\delta)} \tag{15}$$

$f(\alpha)$ is given by Eq. 16:

$$f(\alpha) = \frac{1}{2}(1-\eta)\left(\frac{1}{\cos\alpha} + \left[(1+3\pi/2-2\chi)\sin(\chi+\alpha)-\cos(\chi+\alpha)\right]\sqrt{A} \right) + \frac{m\eta\cos\varphi}{\cos(\alpha+\varphi)}$$

$$-\xi\sin\alpha\left(\frac{(1-\eta)^2}{4}\tan\alpha + \frac{1}{4}\eta(1-\eta)\tan(\alpha+\varphi) + \frac{1}{2}k\eta(1-\eta)\tan(\alpha) + \frac{1}{2}k\eta^2\tan(\alpha+\varphi) \right) \tag{16}$$

$$+\frac{1}{8}\xi(1-\eta)^2 A\sin\chi$$

with $0 \leq \alpha \leq \dfrac{\pi}{2} - \varphi$ and $\chi + \alpha \leq \dfrac{\pi}{2}$

Failure Mechanism II. The second mechanism, shown in Fig. 5, is defined by the zones $A'AGED$ and ACG in translational movement. The lines $A'D$, DE, EG, GC and AG are discontinuity surfaces for the velocity.
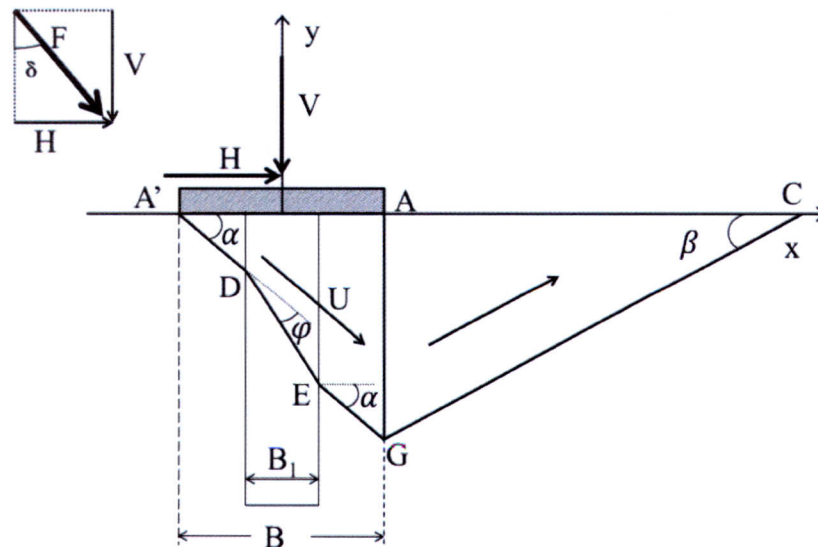

Figure 5. Two translational zones failure mechanism II

The rate of work W_{ex} performed by external forces is obtained by:

$$W_{ex}^{(F)} = UF\sin(\alpha+\delta) + \frac{1}{2}UB^2\gamma_s(1-\eta)\left(\sin\alpha(1-\eta+k\eta)\sqrt{A} - A\cos\alpha \right) \tag{17}$$

with $A = \tan\alpha + \dfrac{\eta\tan(\alpha+\varphi)}{1-\eta}$ and U represents the virtual velocity of volume $A'AGED$ (Fig.5).

On the other hand Eq. 18 presents the maximum rate of work W_{mr} developed for the same velocity field:

$$W_{mr} = CsU(1-\eta)\left(\frac{1}{\cos\alpha} + \left[\sin\alpha + \cos\alpha\tan\beta + \frac{\cos\alpha}{\cos\beta\sin\beta}\right]\sqrt{A} + \frac{m\eta\cos\varphi}{\cos(\alpha+\varphi)(1-\eta)}\right)$$ (18)

Applying Eq. (3) leads to the following inequality:

$$\frac{F}{BC_s} \le \min_{\alpha,\beta}\frac{g(\alpha)}{\sin(\alpha+\delta)}$$ (19)

where

$$g(\alpha) = (1-\eta)\left(\frac{1}{\cos\alpha} + \left[\sin\alpha + \cos\alpha\tan\beta + \frac{\cos\alpha}{\cos\beta\sin\beta}\right]\sqrt{A} + \frac{m\eta\cos\varphi}{\cos(\alpha+\varphi)(1-\eta)}\right)$$
$$-\frac{\xi(1-\eta)}{2}\left(\sin\alpha(1-\eta+k\eta)\sqrt{A} - A\cos\alpha\right)$$ (20)

with $0 \le \alpha \le \dfrac{\pi}{2} - \varphi$.

Failure Mechanism III. The failure mechanism is defined by the rotation of block $A'CDE$ about axis Ωz . The block is delimited by two circular arcs $A'C$ and DE , and the log-spiral curve CD having the focus Ω and angle φ (Fig. 6). This mechanism is similar to the one used by Bouassida and Hadhri (1995), with two differences: for one hand gravity forces are considered in this analysis and for the other, an inclined force is studied.

Similar analysis to those presented for Failure Mechanism I and II was developed, and once again, application of kinematical condition, Eq. (3), yields an upper bound solution of the form

$$\frac{F}{BC_s} \le \min_{\theta_1,\theta_2} g(\theta_1,\theta_2)$$ (21)

where function $g(\theta_1,\theta_2)$ depends on the dimensionless parameters defined in Eq.(1).
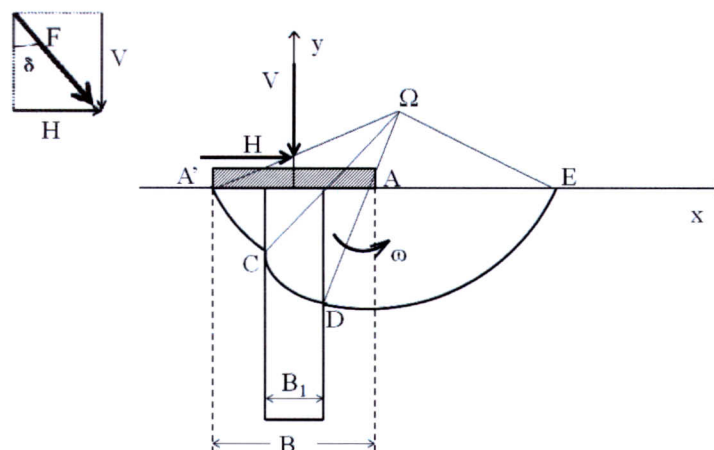
Figure 6. Rotational failure mechanism III

5.2 The Case of a Group of Columns

Failure Mechanism I. The mechanism presented in Fig. 7 consists in a translational motion of the volumes $A'AEG$ and ADC, while the velocity $\underline{U} = U_0\, \underline{e}_\theta$ is constant and orthoradial in the fan AEC This failure mechanism involves velocity jumps along lines $A'GE, AE, CD$ and circular arc EC.
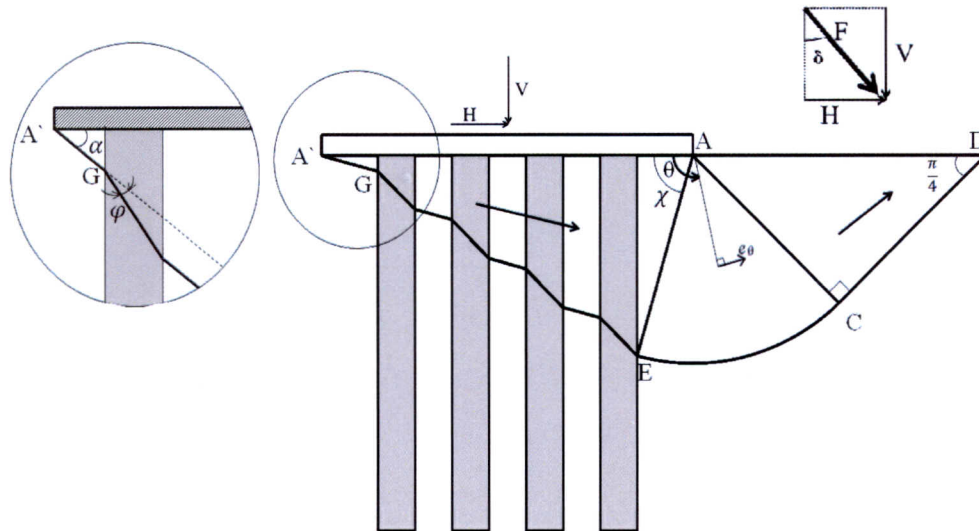

Figure 7. Generalized Prandtl type failure mechanism I

Applying the fundamental kinematic equality Eq. (3), by previously calculating the maximum resisting work (Eq. 4) and the rate of work W_{ex} performed by external forces, an upper bound solution is obtained of the form:

$$\frac{F}{BC_s} \leq \min_\alpha \frac{f(\alpha)}{\sin(\alpha + \delta)} \tag{22}$$

where δ is used to denote the inclination angle of applied load (Fig. 7) and $f(\alpha)$ is given by Eq. 24:

$$f(\alpha) = r\left[\text{sen}(\chi + \alpha)\left(1 + \frac{3\pi}{2} - 2\chi\right) + \cos(\chi + \alpha)\right] + \frac{1 - \eta - a}{\cos\alpha} + \frac{m\eta\cos\varphi}{\cos(\alpha + \varphi)}$$

$$-\xi\sin\alpha\left[\frac{1}{2}\tan\alpha\left(1 - \eta - a\right)^2 + \tan(\alpha + \varphi)\left(\frac{l\eta}{n}\sum_{i=1}^{n-1} i + \frac{1}{2}k\eta^2\right) + \frac{\eta}{n}k\tan\alpha\left(an + l\sum_{i=1}^{n-1}(n-i)\right)\right] \tag{23}$$

$$-\xi\sin\alpha\left[\frac{1}{2}a\left(\eta\tan(\alpha + \varphi) - \tan\alpha\left(1 - \eta - a\right)\right)\right] + \frac{1}{2}\xi r^2\sin(\chi + \alpha)\sin\chi$$

and $r = \sqrt{a^2 + \left[(1 - \eta - a)\tan\alpha + \eta\tan(\alpha + \varphi)\right]^2}$ with conditions: $0 \leq \alpha \leq \frac{\pi}{2} - \varphi$ and $\chi + \alpha \leq \frac{\pi}{2}$

Failure Mechanism II. The second mechanism defined by the zones $A'AGD$ and ACG in translational movement is shown in Fig. 8. The lines $A'D$, DG, GC and AG are discontinuity surfaces for the velocity.
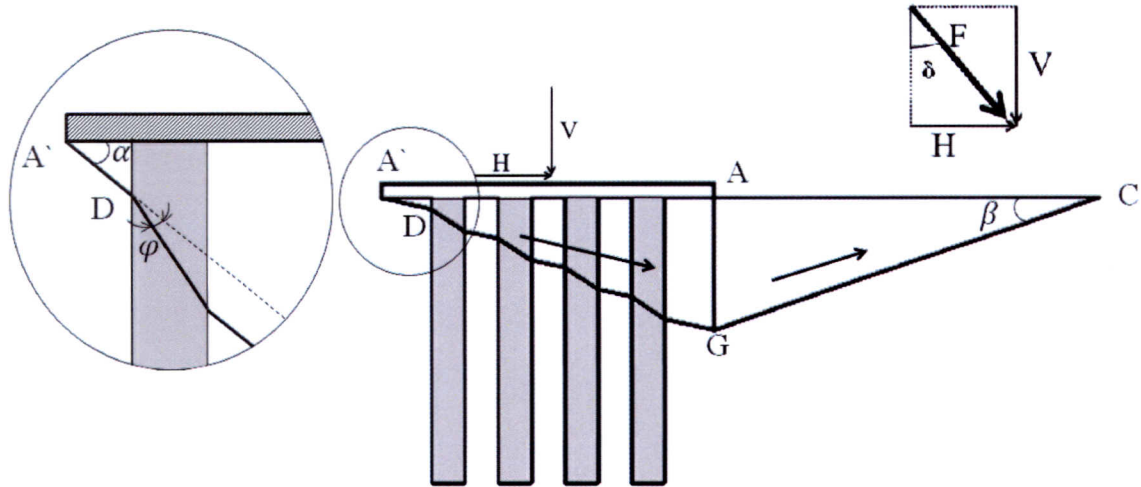
Figure 8. Two translational zones failure mechanism II

The application of Eq. (3) leads to the following inequality:

$$\frac{F}{BC_s} \le \min_{\alpha, \beta} \frac{g(\alpha)}{\sin(\alpha + \delta)} \tag{24}$$

where

$$g(\alpha) = -\xi \operatorname{sen}\alpha \left[\frac{1}{2}\tan\alpha(1-\eta)^2 + \eta\tan(\alpha+\varphi)\left(\frac{l}{n}\sum_{i=1}^{n-1} i + a \right) + \frac{1}{2}k\eta^2\tan(\alpha+\varphi) \right]$$

$$-\xi \operatorname{sen}\alpha \left[ak\eta\tan\alpha + \eta kl\tan\alpha \sum_{i=1}^{n-1}(n-i) \right] + \frac{1}{2}\xi\cos\alpha\left[(1-\eta)\tan\alpha + \eta\tan(\alpha+\varphi) \right]^2 \tag{25}$$

$$+\frac{1-\eta}{\cos\alpha} + \left[(1-\eta)\tan\alpha + \eta\tan(\alpha+\varphi) \right]\left(\sin\alpha + 2\sqrt{2}\cos\alpha \right) + \frac{m\eta\cos\varphi}{\cos(\alpha+\varphi)}$$

with condition: $0 \le \alpha \le \dfrac{\pi}{2} - \varphi$

Failure Mechanism III. The third failure mechanism presented in Fig. 9 is defined by the rotation of block $A'CD$ about axis Ω_z. The block is delimited by circular arcs and log-spiral curves having the focus Ω and angle φ.

Application of kinematical condition, Eq. (3) yields an upper bound solution of the form

$$\frac{F}{BC_s} \le \min_{\theta_1, \theta_2} f(\theta_1, \theta_2) \tag{26}$$

where function $f(\theta_1, \theta_2)$ depends on the dimensionless parameters defined in Eq. (1). A numerical minimization over θ_1 and θ_2 is performed.
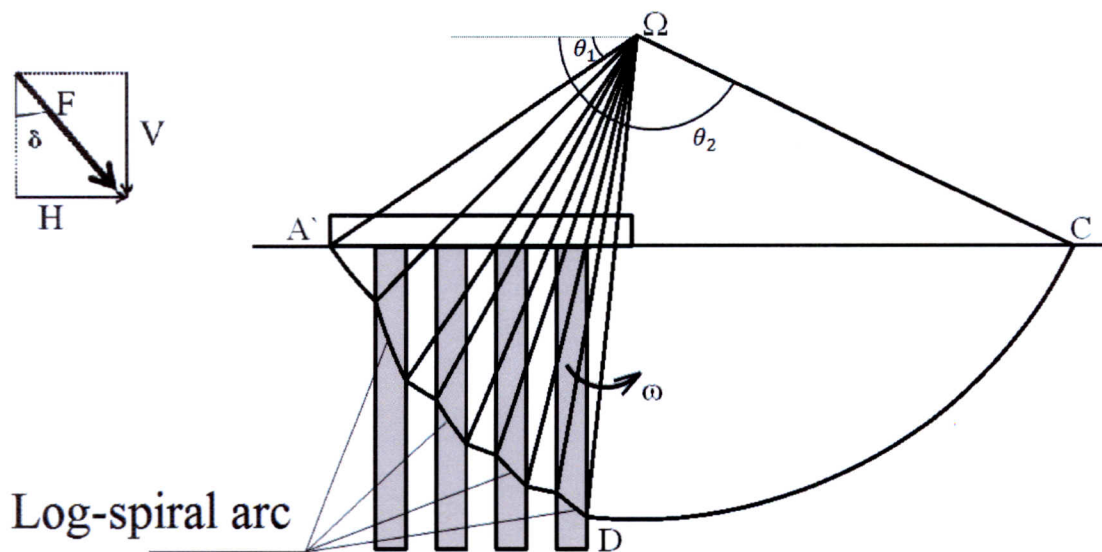
Figure 9. Rotational failure mechanism III

6 RESULTS

6.1 The Case of an Isolated Column

The static approach is defined by the boundary of the surface which, in the space (H,V) or (F,δ), for a fixed set of parameters $\{k,m,\varphi,\xi,\eta,h/B\}$ presented in Eq. 1, delineates the set of safe loads. This method approximates the extreme loads "from inside", while the kinematic approach does it "from outside".

For illustrative purposes, Fig. 10 shows the results obtained in the context of this analysis for a cohesive soil reinforced by a column consisting of original soil blended with lime $(C_r > C_s, \varphi = 0)$.

As it could be expected the reinforcing effect induced by cohesive columns is increasing with ratio C_r / C_s. Unlike the static approach, the kinematic approach predicts improvement of the bearing capacity in both horizontal and vertical directions of the load, thus emphasizing the necessity to resort to more sophisticated stress distributions.

The variation of the lower and upper bound estimate as a function of the cohesion ratio m for a purely vertical load is presented in Fig. 11. The static approach shows that reinforcement occurs from a cohesion ratio $m = 2.6$ and $m = 3.4$ for replacement ratios of $\eta = 0.4$ and $\eta = 0.25$ respectively.

The second application refers to reinforcement by means of purely frictional columns $(C_r = 0, \varphi \neq 0)$. Figure 12 shows the results obtained for two values of the column friction angle. The reinforcement reveals effective only for sufficiently high values of φ. Similarly to the results developed in Salençon and Pecker (1995b), it is also observed that the lower bound estimates tend to zero as the load direction is closer to the horizontal one.
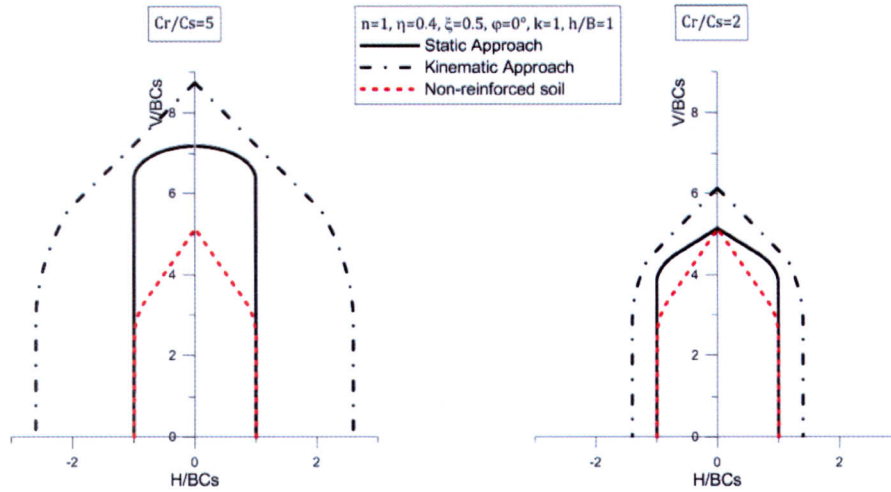
Figure 10. Lower and upper bound approach for the bearing capacity domain for cohesive columns
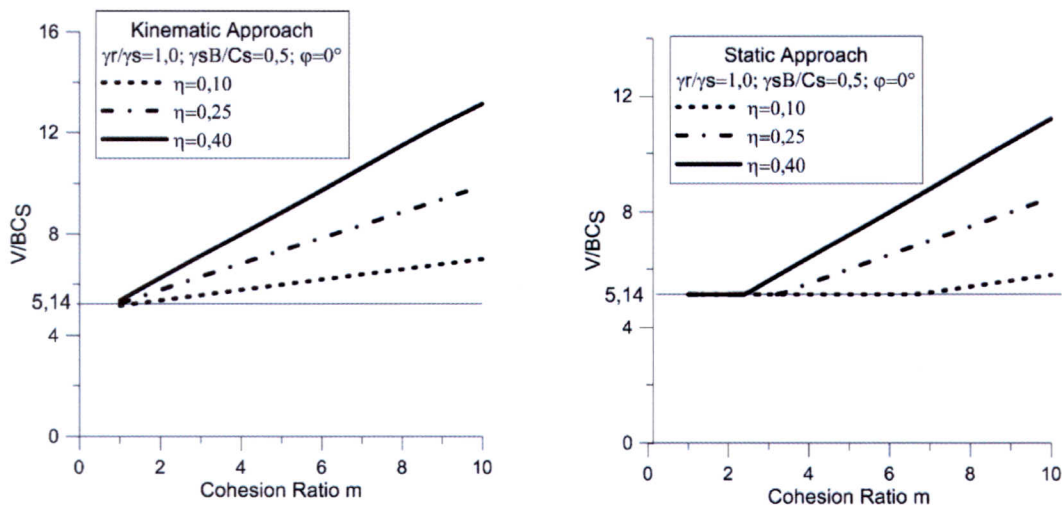

Figure 11. Lower and upper bound approach for the bearing capacity domain of a purely vertical loading for cohesive columns
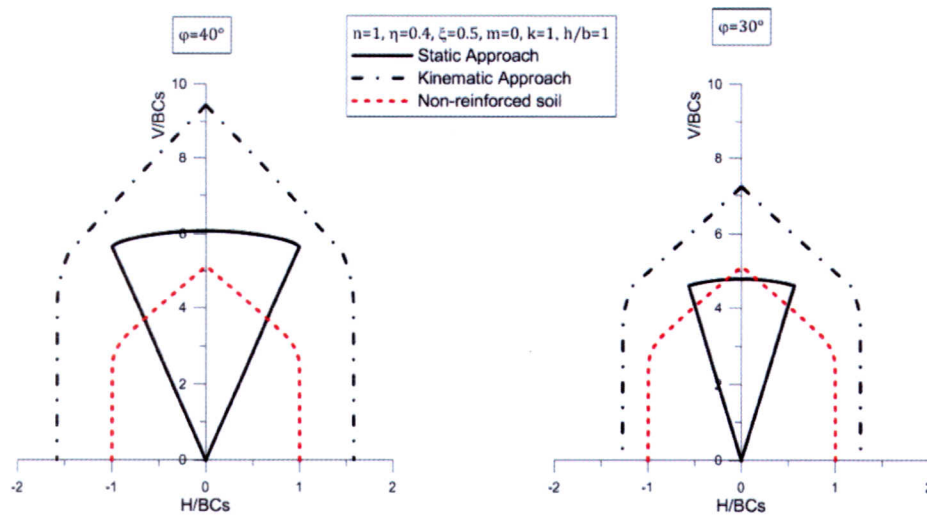

Figure 12. Lower and upper bound approaches for the bearing capacity domain for purely frictional columns

The evolution of the lower and upper bound estimates with friction angle φ is shown in Fig.13 for a purely vertical load V. The static approach indicates that reinforcement occurs from the friction angle $\varphi = 20°$ for a replacement ratio of $\eta = 40\%$, while for 25% it happens from $\varphi = 27°$. The increase of the bearing capacity depends of these two parameters: η and φ.
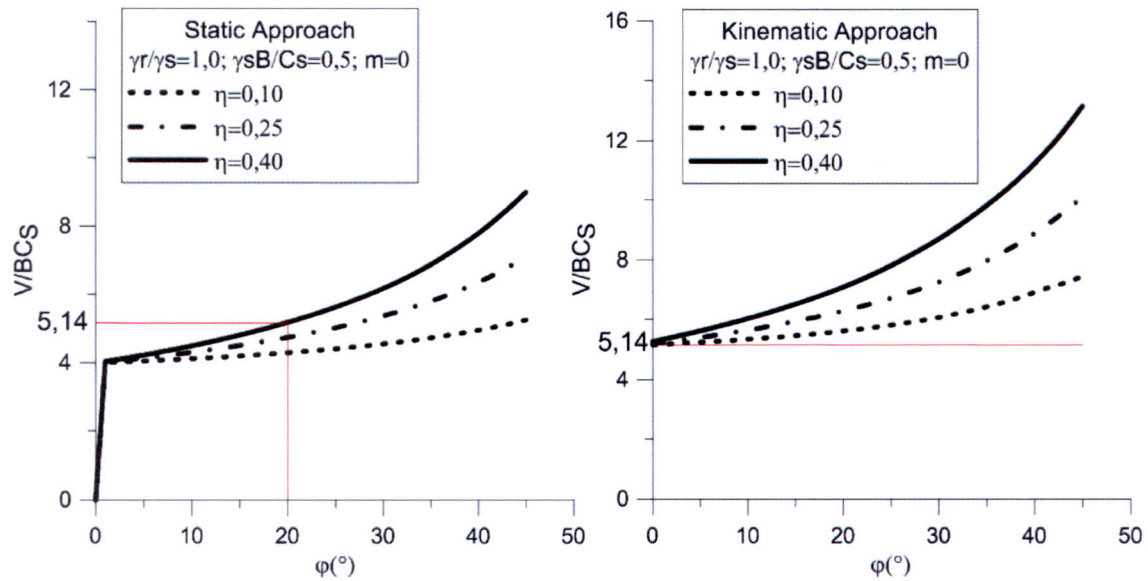

Figure 13. Lower and upper bound approaches for the bearing capacity domain for purely frictional columns

Table 1 summarizes the results obtained in this work and values from Bouassida and Hadhri (1995) for illustrative examples. The static approach given by these authors corresponds to a particular case of the stress field considered in this work (when $\alpha = 0°$ and gravity is neglected), therefore, same values of the lower bound were obtained. As regard to the upper bound, better estimations of the limit load were founded in comparison with Bouassida and Hadhri (1995).

Table 1. Results for a purely frictional column material

η	Lower Bound by the static approach		Lower Bound by Bouassida and Hadhri (1995)		Upper Bound by Bouassida and Hadhri (1995)		Upper Bound by the kinematic approach	
	$\varphi = 25°$	$\varphi = 30°$	$\varphi = 25°$	$\varphi = 30°$	$\varphi = 25°$	$\varphi = 30°$	$\varphi = 25°$	$\varphi = 30°$
0.2	4.18	4.40	4.19	4.40	5.99	6.32	5.71	6.07
0.4	4.37	4.80	4.37	4.80	6.51	7.21	6.37	7.07
0.6	4.56	5.20	4.56	5.20	7.11	8.25	7.11	8.25

6.2   The Case of a Group of Columns

In the same form adopted in the previous section, two categories of column materials are subsequently studied. The combination of static and kinematic approaches provides lower and upper bounds domains for the bearing capacity for each category. An illustrative example of such approaches for a purely cohesive column material $(C_r > C_s, \ \varphi = 0)$ is first presented. Figure 14 relates the extreme non dimensional external force $\dfrac{F}{BCs}$ with the inclination angle δ of the load. Both the static and kinematic approaches predict an improvement of the extreme load for inclination angles between $0 \le \delta \le 20°$. The interaction between the non-dimensional load components of the upper and lower bound estimates (Fig. 14) shows that an increase on the horizontal component of the force implies a reduction of the vertical bearing capacity.
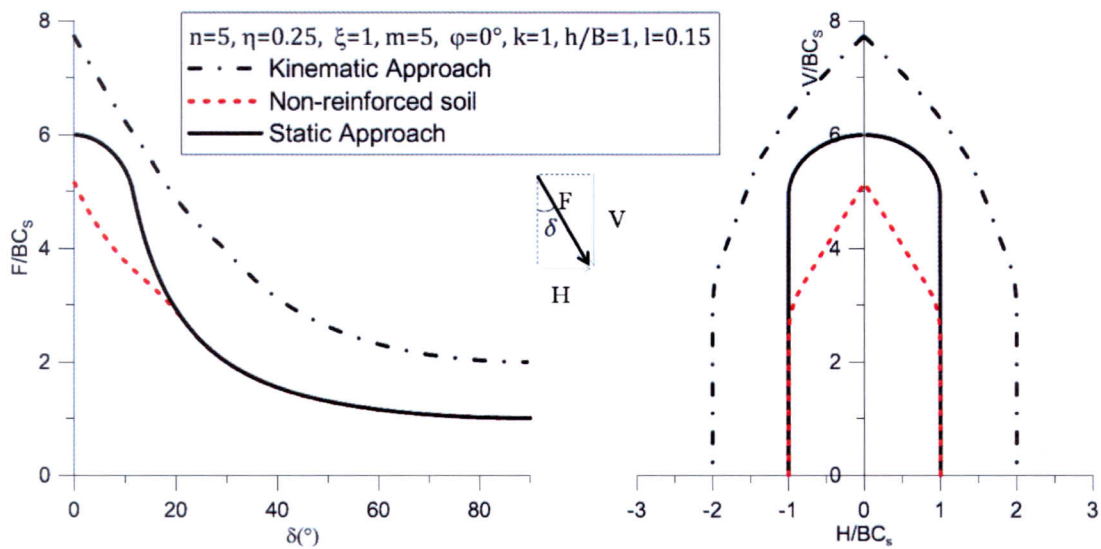

Figure 14. Lower and upper bound estimates for the bearing capacity domain for purely cohesive columns

Figure 15 refers to reinforcement by means of purely frictional columns $(C_r = 0, \ \varphi \ne 0)$. The lower and upper bound estimates are compared to the ultimate bearing capacity of a non-reinforced soil in Fig.15 relating the Force $\dfrac{F}{BCs}$ to its inclination angle δ. Results are conveniently presented in the plane $\left(\dfrac{H}{BCs}, \dfrac{V}{BCs} \right)$ in Fig. 15 as the lower and upper domains of the extreme loads. For both categories of material reinforcement, the ultimate bearing capacity could only be bracketed. Generally, upper bound estimates lead to better approximations of the bearing capacity, therefore, more sophisticated stress distributions should be considered in order to conceal extremes loads boundaries with a higher degree of accuracy.
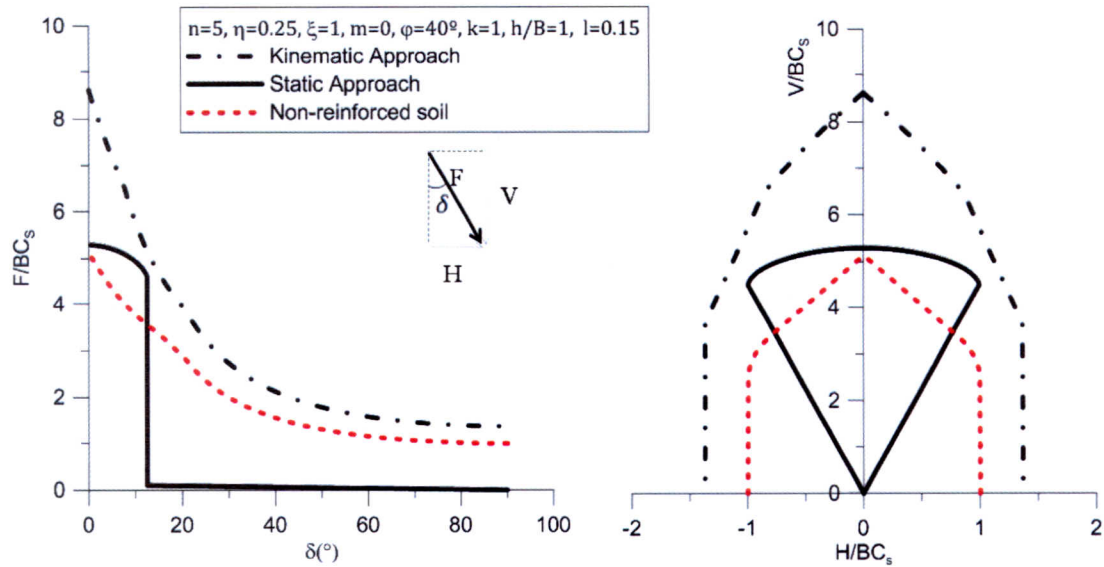
Figure 15. Lower and upper bound approach for the bearing capacity domain for purely frictional columns

Analytical and elastoplastic simulations were performed by Hassen G. et al (2013) based on a periodic homogenization limit analysis method to determine the homogenized strength capacity of column reinforced soil. Upper bound estimates of the ultimate bearing capacity using the previously obtained numerical estimate of the strength domain for a purely vertical load in plane strain analysis have been derived. Table 2 compares this result with the upper and lower bound studied in this work for the fixed set of parameters: $\{n=6,\ \eta=0.28,\ \varphi=35°,\ k=0,\ \xi=0,\ m=0,\ l=0.15\}$. The difference between these upper bounds is 4%.

Table 2. Results for a group of purely frictional column material

Lower Bound by the Static Approach	Upper Bound by Hassen G. et al (2013) using homogenization approach and yield design theory	Upper Bound by the Kinematic Approach
5.01	7.15	7.76

7   CONCLUSIONS

The problem solved in the current study, relates to the ultimate bearing capacity of a strip footing resting on the surface of a column reinforced soil subjected to an inclined, central load. The extreme load is defined within the framework of the plane strain yield design theory using the yield strengths of the materials involved. Both lower and upper bound solution have been derived in the situation of a single column and of a group of columns.

The novelty of this contribution is in its ability to deal with inclined loads situation. The analysis may be viewed as a generalization of existing approaches developed in the case of vertical loading. The results bracket the variations of the bearing capacity as a function of

either the load inclination or the column and soil strength parameters. The interaction between the load components showed that as soon as the horizontal component of the force increases, the vertical component of the bearing capacity decreases. This aspect should thus be carefully considered in foundation design.

The foundation ultimate bearing capacity has been compared with available solutions derived for purely vertical load.

REFERENCES

Bouassida M., Hadhri T., 1995. Extreme load of soils reinforced by columns: the case of an isolated column. *Soils and Foundations* vol. 35, pp. 21-35.

Bouassida M., Jellali B. & A. Porbaha, 2009. Limit analysis of rigid foundations on floating columns. *International Journal of Geomechanics* vol. 9, pp. 89-101.

Datye, K. R., Madhav, M. R., 1988. Case histories of foundations with stone columns. *Second International Conference on Case Histories in Geotechnical Engineering,* pp. 1075-1086.

Hassen G., Gueguin M., de Buhan P., 2013. A homogenization approach for assessing the yield strength properties of stone column reinforced soils. *European Journal of Mechanics A/Solids.,* vol 37, pp. 266-280.

Jellali B., Bouassida M. & de Buhan P, 2005. A homogeneization method for estimating the bearing capacity of soils reinforced by columns. *International Journal for numerical and analytical methods in geomechanics.* vol. 29, pp. 989-1004.

Jellali B., Bouassida M., de Buhan P., 2007. A homogenization approach to estimate the ultimate bearing capacity of a stone column reinforced foundation. *International Journal of geotechnical engineering,* vol. 1, pp. 61-69.

Nazari J., Ghazavi M., 2012. A simple analytical method for calculation of bearing capacity of stone-column. *International Journal of Civil Engineering,* vol. 1, pp. 15-25.

Prandtl L., 1923. Anwendungbeispiele zu einem Henckyshen Satz über das plastiche Gleischgewicht, Z. Angew. *Math. Mech.,* vol. 3, pp. 401.

Salençon J., 1990. An introduction to the yield design theory and its applications to soil mechanics. *European Journal of Mechanics – A/Solids,* vol. 9, pp. 447-500.

Salençon J., Pecker A., 1995. Ultimate bearing capacity of shallow foundations under inclined and eccentric loads. Part I: purely cohesive soil. *European Journal of Mechanics-A/Solids,* vol 3, pp. 349-375.

Salençon J., Pecker A., 1995b. Ultimate bearing capacity of shallow foundations under inclined and eccentric loads. Part II: purely cohesive soil without tensile strength. *European Journal of Mechanics-A/Solids,* vol 3, pp. 349-375.

Schaefer, V. R. Ground improvement, ground reinforcement, ground treatment. Developments 1987-1997, 1997. *Proceedings of Soil Improvement and Geosynthetics of the Geo-insitute of the American Societey of Civil Engineers in Conjunction with Geo-Logan'97.* pp. 75 and 102.

CILAMCE 2015

Proceedings of the XXXVI Iberian Latin-American Congress on Computational Methods in Engineering
Ney Augusto Dumont (Editor), ABMEC, Rio de Janeiro, RJ, Brazil, November 22-25, 2015